PHYSICAL ANALYSIS OF SWIRLING JETS BY MEANS OF PSEUDO-SPECTRAL METHOD

Ana Marta de Souza, amsouza@mecanica.ufu.br
Universidade Federal de Uberlândia – Av. João Naves de Ávila, 2160. Campus Santa Mônica. Uberlândia-MG
Francisco José de Souza, francisco.souza@embraer.com.br
EMBRAER Empresa Brasileira de Aeronáutica SA – Av. Brigadeiro Faria de Lima, 2170. São José dos Campos-SP
Aristeu da Silveira Neto, aristeus@mecanica.ufu.br
Universidade Federal de Uberlândia – Av. João Naves de Ávila, 2160. Campus Santa Mônica. Uberlândia-MG

Abstract. *Swirling jets have commonly numerous practical aplications like supersonic combustor, cyclone separators, systems of mixing and propulsion. A better understanding of the generation and evolution mechanisms is necessary for engineering and theoretical interests. The present work consists in the physical analysis of a swirling jet by means of three-dimensional simulations using a pseudo-spectral method. The detailed structures of the flow could be visualized and their mechanisms explained. A comparison of the swirling and natural jets were carried out. The possibility of controlling jet though the imposition of different perturbations to the initial conditions could be cofirmed, as already performed in recently works, in which other kinds of jets were studied. The proximity of the inertial region to the inclinations of -5/3 and the decay region were verified in the energy spectra.*

Keywords*: pseudo-spectral method, turbulence transition, swirling jet, natural jet*

1. INTRODUCTION

The interest in the study of swirling jets is justified due their great practical applications, such as supersonic combustors, cyclone separators, systems of mixing and propulsion. Nowadays, many studies have been carried out on the instability and dynamic of the three-dimensional flow structures. The improvement of understanding of structures generation and evolution mechanisms should contribute to optimization of engineering systems and refinement of existent theories and models.

The optimization of the jet applications should be obtained through the manipulation of the “coherent structures, which are responsible to influence strongly the jet dynamic especially in the transition turbulence near the jet inlet. In the numerical solutions, the imposition of different initial perturbations offers the possibility to control the flow dynamic. In practical terms, the passive control refers to control of the jet spatial evolution through the use of particular shapes of the inlet nozzle (Gutmark e Gristein, 1999). The active control refers to deterministic perturbation at the jet inlet created through energy consuming devices, which can be obtained, in practice, through the use of loud-speakers (Crow and Champagne, 1971; Zaman and Hussain, 1980) or flap actuator (Zaman et al, 1994; Suzuki et al., 2000).

According to Hu and Yin (2001) there are many works in the literature which employ different kinds of swirl models, comparison between experimental and theoretical results and different numerical methodologies. Those authors, in order to clarify some issues, performed a Direct Numerical Simulation (DNS) of a swirling jet near the outlet of a nozzle with axisymetric and non-symmetric disturbances to investigate the dynamic of the flow.

The present work has the main goal similar to that of Ho and Yin (2001), who present interesting results. However, in the present work, the authors concentrated the study in the physical analysis, detailing the structures of flow, showing the typical phenomena and comparing the results with those of the natural jet. The methodology employed was the pseudo spectral method, differently of Ho and Yin (2001), whose utilized finite-difference. The pseudo-spectral methodology was chosen due the advantages, such as computational economy, high accuracy and the easy implementation, according observed by the authors in previous works (Souza et al., 2005).

2. GOVERNING EQUATIONS AND NUMERICAL METHOD

The Navier-Stokes and continuity equations with constant physical properties that describe the incompressible jet flow are:

$$\begin{cases} \dfrac{\partial u_i}{\partial t} + \dfrac{\partial}{\partial x_j}\left(u_i u_j\right) = -\dfrac{\partial p}{\partial x_i} + \nu \dfrac{\partial^2 u_i}{\partial x_j \partial x_j} \\ \dfrac{\partial u_i}{\partial x_i} = 0 \end{cases} \tag{1}$$

The governing equations can be written in the spectral space:

$$\begin{cases} \dfrac{\partial \hat{u}_\ell}{\partial t} + \nu\, k^2 \hat{u}_\ell = -i k_m P_{jm}\left(\vec{k}\right) \displaystyle\int_{\vec{p}+\vec{q}=\vec{k}} \hat{u}_\ell\left(\vec{p}\right) \hat{u}_j\left(\vec{q}\right) d\vec{p} \\ i\vec{k} \cdot \hat{\vec{u}} = 0 \end{cases} \tag{2}$$

The Navier-Stokes equations do not dependent on the pressure concept in Fourier space, contrary to what happens in the physical space. The resolution of non-linear convolution integral that appears on Eq. (2) is impractical due to its high computational cost. For this reason, the methods named pseudo-spectral have been used. These methods consist in solving the product of velocities in physical space and transforming them to Fourier space, in which the derivatives are computed. Thus, the transformed velocity field is computed, the inverse transform calculated and the velocity field in the physical space determined.

The SPECTRAL code, which was developed by the authors, employees a pseudo-spectral method to solve the Navier-Stokes equations in spectral space, which can be rewritten in the following form for the three flow directions:

$$\frac{\partial \hat{u}}{\partial t} = -\hat{H}_{u_\pi} + \nu\left(-k_x^2 - k_y^2 - k_z^2\right)\hat{u}\,, \tag{3}$$

$$\frac{\partial \hat{v}}{\partial t} = -\hat{H}_{v_\pi} + \nu\left(-k_x^2 - k_y^2 - k_z^2\right)\hat{v} \tag{4}$$

$$\frac{\partial \hat{w}}{\partial t} = -\hat{H}_{u_\pi} + \nu\left(-k_x^2 - k_y^2 - k_z^2\right)\hat{w}\,, \tag{5}$$

where $\hat{u}$, $\hat{v}$ e $\hat{w}$ are the Fourier coefficients for the velocities u, v e w, respectively; and $\hat{H}_{u_\pi}$, $\hat{H}_{v_\pi}$ e $\hat{H}_{w_\pi}$ represent the advective terms in each equation projected into the π plane.

Equations (3), (4) and (5) were advanced in time with the Adams-Bashforth and Runge-Kutta schemes, both of 3rd order. After the two initial time steps with the 3rd-order Runge Kutta scheme (RK3), the temporal advance employs the 3rd-order Adams Bashforth scheme (AB3). At each time step or sub-step the transformed Navier-Stokes equations are solved.

At the moment, only periodic boundary conditions are available in the SPECTRAL code.

2.1. Initial Conditions

The jet flow simulations were performed at Reynolds number 1600, time step 0.005 s and 120^3 Fourier modes in a cubic domain of dimensions *8R x 8R x 8R*, where *R* is the initial radius, as shown in Fig. 1.

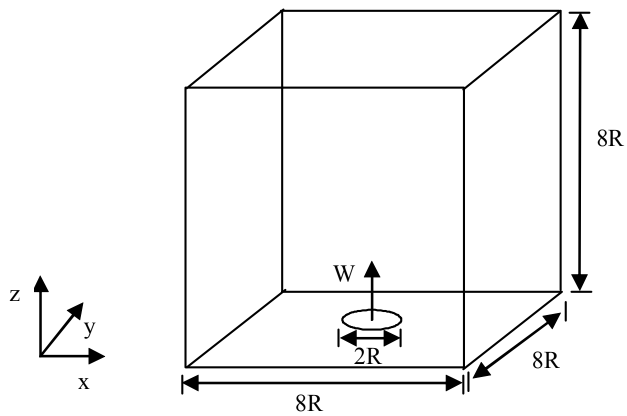

Figure 1. Scheme of computational domain.

The initial axial velocity profile is chosen so as to mimick a tubular mixing layer. According to literature and preliminary tests carried out by the authors, a hyperbolic tangent velocity can reflect the basic physical features of the flow. The initial velocity condition is presented by Equation 6.

$$w_0(r,\theta,z,0)=\begin{cases} 1 & (r \le R-\delta) \\ \frac{1}{2}\cdot\left[1-\tanh\left(\frac{r-R}{2\delta}\right)\right] & (R-\delta < r < R+\delta), \\ 0 & (r \ge R+\delta) \end{cases} \quad (6)$$

where r is given by $r=\sqrt{x^2+y^2}$, with reference in the Cartesian system coordinate, R is the initial jet radius and δ is the characteristic half-width of the shear layer, equal to 2.5/16 m.

3. SIMULATION RESULTS

3.1. Swirling Jet

The Lam-Oseen vortex profile in the azimuthal direction is the basic flow model that characterizes the "swirling jet". In rectangular coordinates, the profile is presented by the components velocity as follow:

$$u=-0.2\cdot y\cdot\left[1-e^{\left(\frac{-r^2}{0.05}\right)}\right] \quad \text{and} \quad v=0.2\cdot x\cdot\left[1-e^{\left(\frac{-r^2}{0.05}\right)}\right] \quad (7)$$

The axial disturbance and the modified transversal velocities are presented, respectively, by the follow equations:

$$U_r=0,01\cdot sen\left(2\pi\frac{z}{4.0}\right)+0,02\cdot sen\left(2\pi\frac{z}{2.0}\right)+0,03\cdot sen\left(2\pi\frac{z}{1.0}\right)\cdot \quad (8)$$

$$u_r=u+U_r\cdot\frac{x}{r}\cdot e^{\left[-2,0\cdot\left(\frac{r-R}{2\delta}\right)^2\right]} \quad \text{and} \quad v_r=v+U_r\cdot\frac{y}{r}\cdot e^{\left[-2,0\cdot\left(\frac{r-R}{2\delta}\right)^2\right]} \quad (9)$$

a) Visualization of flow structures

Figure 2 presents the temporal evolution by means of the criterion Q isosurfaces in the 0.01 s^{-2} level.

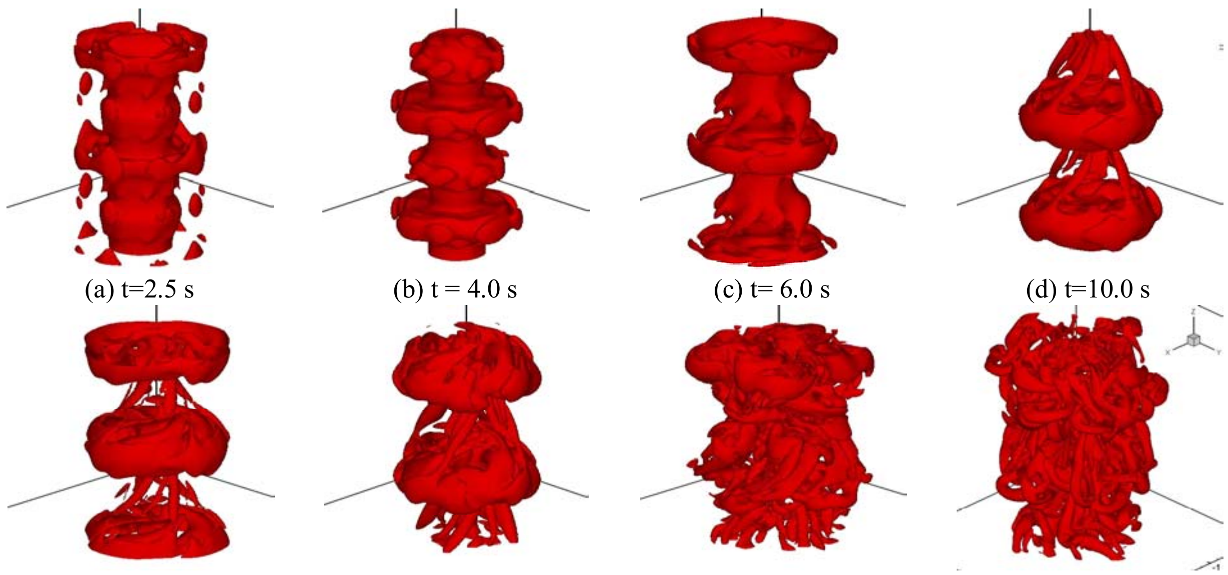

(a) t=2.5 s (b) t = 4.0 s (c) t= 6.0 s (d) t=10.0 s
(e) t = 12.5 s (f) t = 15.0 s (g) t = 20.0 s (h) t = 30.0 s

Figure 2. Criterion Q temporal evolution (Isosurface level = 0.01 s^{-2}) - Swirling Jet.

Observing Fig. 2, it is possible to verify the preliminary formation of rings due to primary harmonic mode (a, b, c). From (c) to (d), the rings are better detailed and are connected through filaments. The influence of perturbation can be observed, especially in the filaments that connect the rings, which seem to be twisted in azimuthal direction. The azimuthal mode grows in the subsequent instants (e) and the filaments that connect rings are more thin and twisted than before. At the same time that the rings are being advected due the linear mode, the twist moving happens. In (f), the interaction between primary (rings) and secondary (filaments) structures became more pronounced, begging the rings deformation. In (g) the azimuthal instability is observed, the rings do not exists more, the interaction between structures is greater than instants before, breaking down quickly to a disordered (turbulence) state (h).

More details of flow structures can be observed through Figures 3 and 4, which show the vorticity field in temporal evolution in planes xz and xy, respectively.

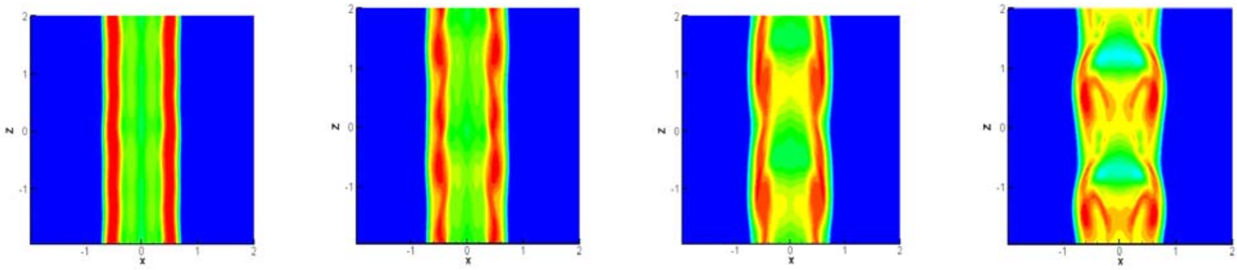

(a) t= 2.5 s (b) t= 4.0 s (c) t= 7.5 s (d) t= 10.0 s

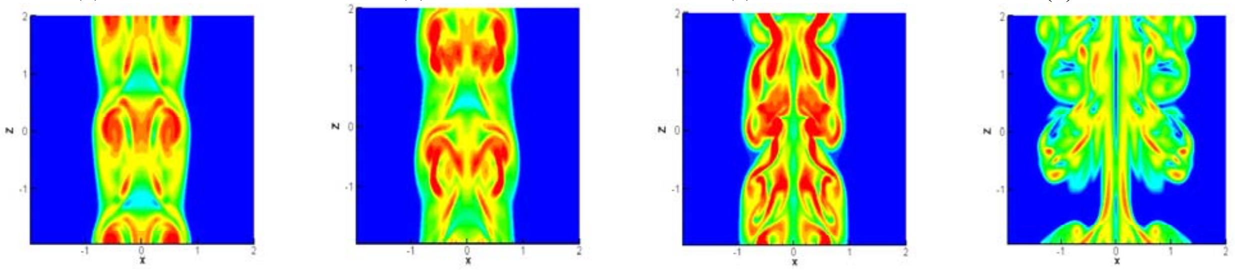

(e) t= 12.5 s (f) t= 15.0 s (g) t= 20.0 s (h) t= 30.0 s

Figure 3. Vorticity $\|\vec{\omega}\|$ in temporal evolution in the plane xz (y=0) – Swirling Jet.

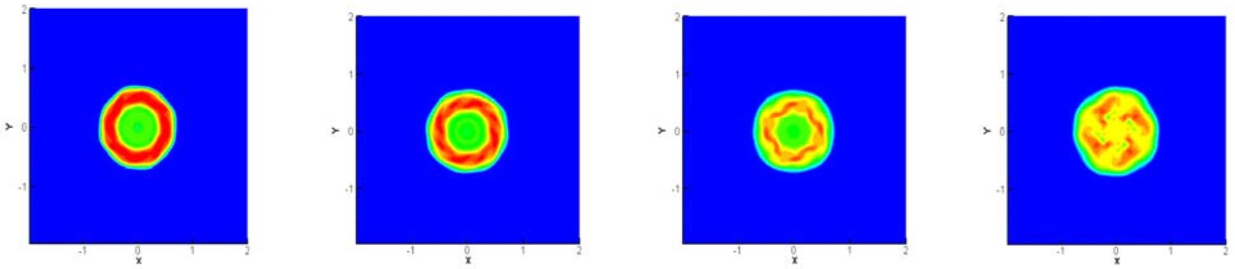

(a) t= 2.5 s (b) t= 4.0 s (c) t= 7.5 s (d) t= 10.0 s

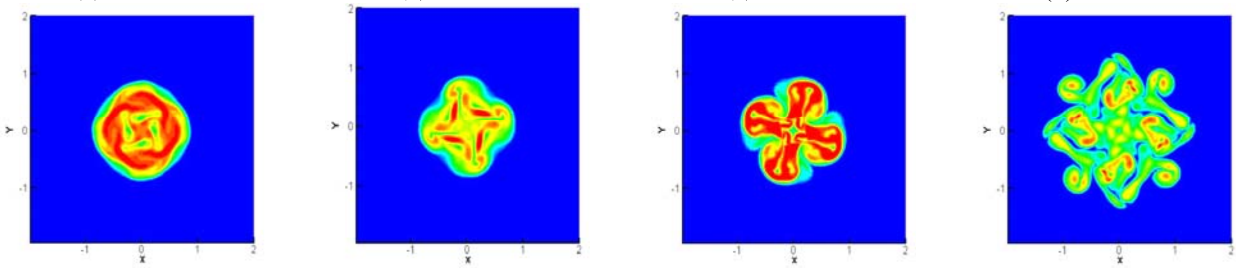

(e) t= 12.5 s (f) t= 15.0 s (g) t= 20.0 s (h) t= 30.0 s

Figure 4. Vorticity $\|\vec{\omega}\|$ in temporal evolution in the plane xy (z=0) – Swirling Jet.

According to Hu and Yin (2001), a negative azimuthal vorticity appears and the relatively weak vortex structures with negative vorticity are being strengthened under the continuous interaction between the primary vortex ring and the columnar vortex. This phenomenon causes the formation of a secondary vortex ring with opposite vorticity. The vortex core region is stretched under the action of the vortex ring formed in the vortex pairing process, and erupts deeply into the mixing layer. The flow field is dominated by the motion of a pair of vortex rings. The two rings induce each other just like a pair of vortex rotating in the opposite direction, and produce a positive radial velocity in the cross plane. Figs. 3 and 4 present an interesting symmetric behavior in relation to a central line all the time.

Figure 3 shows the rolling up of mixing layer (a) and the formation of vortex rings in the field flow (3 b). The vortex paring is identified in Fig 3c. Some typical phenomena of the swirling jet can be observed in the visualizations: the rolling-up of vortex in the core region (Fig 3d and Fig 4d), vortex stretching under the action of vortex rings formed (Fig 3 e and Fig 4 e), the strengthening of interactions between primary and secondary structures (Fig. 3f, g and Fig 4 f, g), small eddies composing the flow (Fig 3h and Fig.4 h). The outward radial motion, noted by Park et all (1998) in their axisymetric computations, is observed in Fig. 3(f) to (h) and Fig 4 (f) to(h). The secondary counter-rotating vortex is identified in Fig. 4h. These vortex was also observed by Martin and Meiburg (1998) in their swirling jet model, which is different that employed in the present work.

3.2. Comparison of the Swirling Jet with Natural Jet

In order to observe the swirl effect over the jet dynamic, the flow structures of swirling jet was compared with those of the natural jet. The natural jet is characterized for the imposition of a white noise disturbance:

$$w(x,y,z,t) = w_0(x,y,z,0) + \left(\frac{0,5-a}{100,0} \right) \tag{10}$$

where a is a random number between 0 and 1. The profile of axial component of velocity was previous presented by Eq.(6).

Figures 10 show the different structures evolution in the natural and swirling jets at similar time instants.

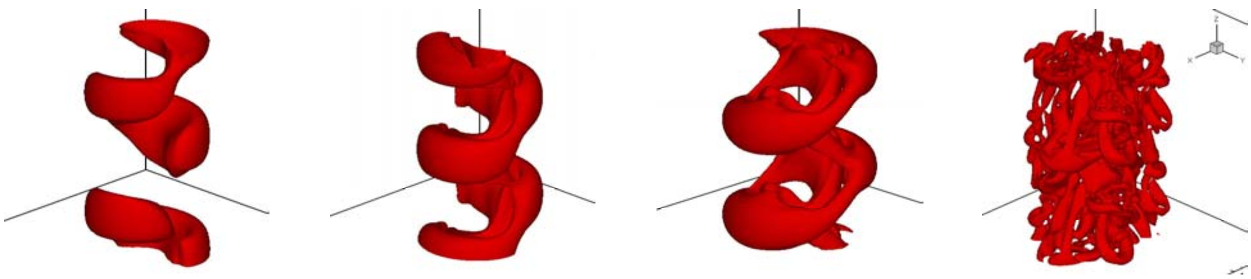

t= 10.0s t=15.0 s t=20.0s t= 30.0s

a) Criterion Q isosurfaces (level = 0.01 s^{-2}) – Natural Jet

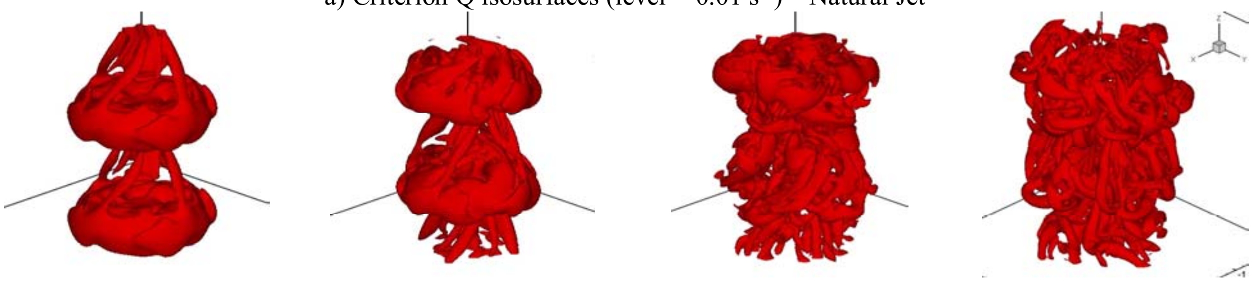

t= 10.0s t=15.0 s t=20.0s t= 30.0s

b) Criterion Q isosurfaces (level= 0.01 s^{-2}) – Swirling Jet

Figure 10. Comparison of temporal evolution through criterion Q isosurfaces between Natural and Swirling jets.

The swirling jet presents faster transition to turbulence than the natural jet. The structures and their evolution are clearly different. The natural jet, which mechanism was already explained by Silva and Metais (2002) and verified by Souza et al.(2005), presents two consecutives rings that connect to form the alternated pairing (Urbin and Metais, 1997). Spanwise filaments are formed by the vortex stretching, and interact with previous instabilities forming the disordered state. The swirling jet presents vortex pairing, but they are no presence of alternated pairing. The results show that the swirl has a little influence on the evolution off the flow in the early stage. Observing the position of rings in times t=10.0 s and t= 15.0 for both cases, the linear mode growing in the swirling jet seems to be slightly smaller than that of the natural jet. Then, the swirl seems to be responsible for the more quickly transition to turbulence in the swirling jet.

Figures 11 and 12 present the vorticity module of the natural and swirling jet, in order to complement the comparison of the flow structures evolution.

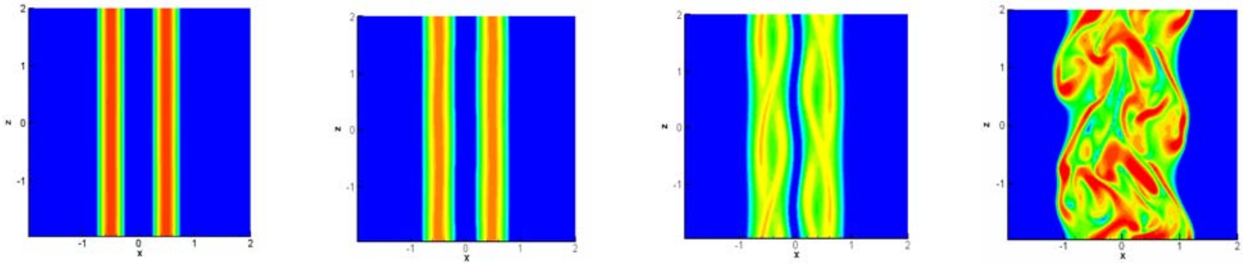

t= 5.0s t=10.0 s t=20.0s t= 30.0s.

a) Vorticity $\|\vec{\omega}\|$ in temporal evolution in the plane xy (z=0) – Natural Jet

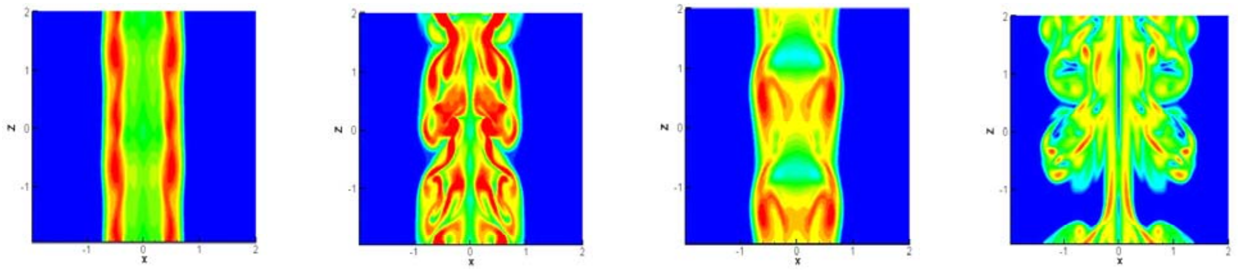

t= 5.0s t=10.0 s t=20.0s t= 30.0s

b) Vorticity $\|\vec{\omega}\|$ in temporal evolution in the plane xy (z=0) – Swirling Jet

Figure 11. Comparison of temporal evolution through Vorticity $\|\vec{\omega}\|$ in temporal evolution in the plane xy between Natural and Swirling Jets.

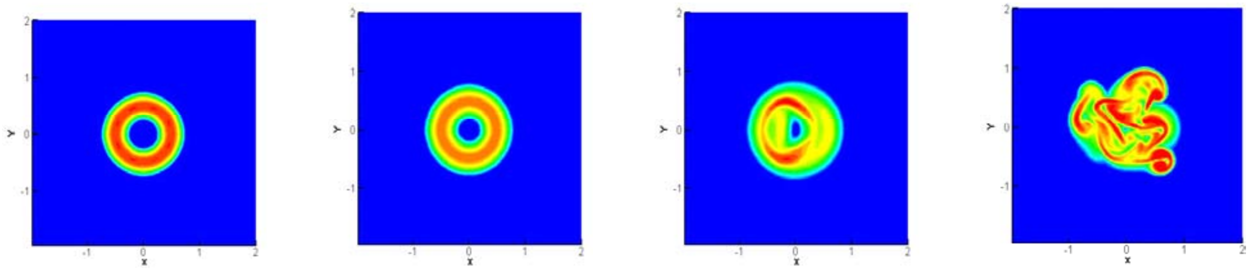

t= 5.0s t=10.0 s t=20.0s t= 30.0s

a) Vorticity $\|\vec{\omega}\|$ in temporal evolution in the plane xz (y=0) – Natural Jet

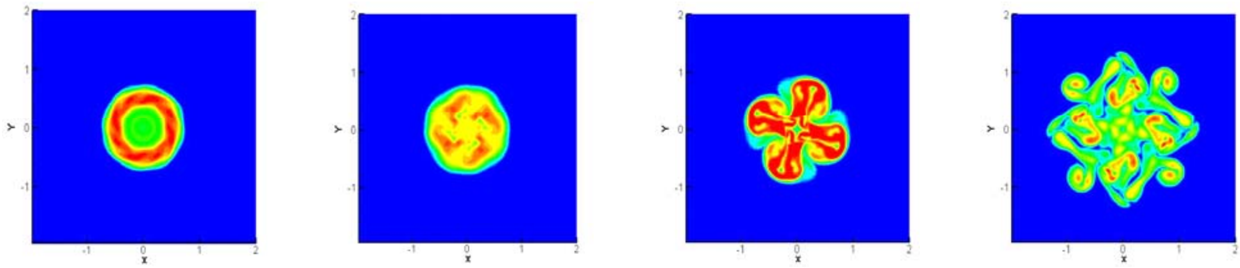

t= 5.0s t=10.0 s t=20.0s t= 30.0s

b) Vorticity $\|\vec{\omega}\|$ in temporal evolution in the plane xz (y=0) – Swirling Jet

Figure 12. Comparison of temporal evolution by means of Vorticity $\|\vec{\omega}\|$ in temporal evolution in the plane xz between Natural and Swirling jets.

The effect of swirl is really noted in the first stages (t=5.0 and t- 10.0 s). The symmetric behavior observed in the swirling jet structures is not observed in the natural jet. This symmetry probably is a result of the evolution mechanisms of swirl. There is no similarity between swirling and natural jet structures, except in the initial stages, when the process of rolling up and vortex pairing is taking place. The different evolution mechanisms suggest the possibility of jet control through the imposition of distinct disturbances, which was already investigated by Souza (2005).

The spectrum of turbulent kinetic energy for the natural and swirling jets are showed at different instants of time in Fig. 11.

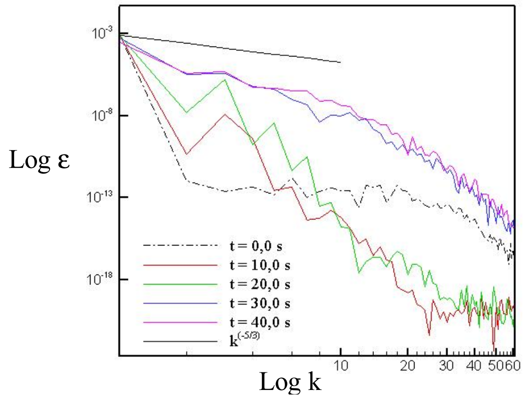

(a) Natural jet

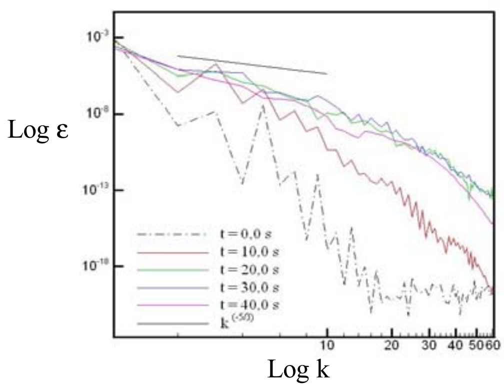

(b) Swirling jet

Figure 11. Turbulent Kinetic Energy Spectrum for Natural and Swirling Jets.

The energy spectrum of natural jet in the range log(k) equals 3 to 10 approach the inclination of -5/3 after 30 seconds. From log(k) equals 10 the decay of kinetic turbulent energy is observed, which is expected for the free jet in temporal development. Similar behavior is verified for the swirling jet. However, from 20 seconds the spectrum already approaches the (-5/3) inclination, probably due the quick transition to turbulence.

Unfortunately, the jet simulation in temporal development does not allow an accurate comparison with experimental data. However, good agreement between structures in a qualitative comparison with experimental data was observed by the authors for the simulated natural jet (Souza et al., 2005). The analogy between temporal and spatial analyses of flow allows to perform some inferences about spatial evolution with base in their temporal evolution. The same evolution phases verified in the spatial development can be identified at different times of temporal development, according showed by Souza (2005).

4. CONCLUSIONS

The physical analysis of swirling jet employing the pseudo-spectral method was performed with success. The influence of swirl was well evidenced. Some phenomena, reported for other authors, was also observed in the present work, such as the rolling-up of vortex in the core region, vortex stretching under the action of vortex rings formed, small eddies composing the flow, outward radial motion and the secondary counter-rotating vortex.

The comparison between natural and swirling jet presented interesting results. The swirl has a little influence on the evolution off the flow in the early stage, when there is similarity between natural and swirling jets. After this stage, the evolution mechanisms are different and the swirl seems to be responsible for the more quickly transition to turbulence in the swirling jet. The symmetric behavior observed in the swirling jet structures is not observed in the natural jet.

5. REFERENCES

Crow, S.C. and Champagne, F.H., 1971, “Orderly structure in jet turbulence”, Journal Fluid Mechanics, 48, 547.

Gutmark, E.J. and Grinstein, F.F., 1999, “Flow control with noncircular jets”, Annu. Rev. Fluid Mech., 31, 239.

Hu, G.H.; Sun, D.J. and Yin, X.Y., 2001. “A numerical study of dynamics of a temporally evolving swirling jet.” Physics of Fluids, vol.13, n. 4, pp. 951.

Martin, J. and Meiburg, E. 1998. “The growth and nonlinear evolution os helical disturbances in a swirling jet model.” Eur. J.Mech. B/ Fluids 17, 639.

Narasimha, R.1990, “The utilities and drawbacks of traditional approaches”. In Whither Turbulence. Turbulence at the crossroads (ed. J.L.Lumley), pp.12-48. Springer.

Park, T. W., Katta, V. R. and Aggarwal., 1998. “On the dynamics of a two-phase, nonevaporing swirling jet.” Int. J. Multiphase Flow24, 295.

Silva, C.B. and Métais, O., 2002. “Vortex control of bifurcating jets: A numerical study.” Physics of Fluids, 2002, Vol. 14, n. 11, pp. 3798-3818.

Souza, A. M., 2005. “Análise Numérica da Transição à Turbulência em Escoamentos de Jatos Circulares Livres.” Tese de Doutorado. Universidade Federal de Uberlândia.

Souza, A.M.; Souza, F.J. and Silveira-Neto, A., 2005. “Numerical Simulation of the Turbulent Transition in Free Round Jets.” Proceedings of COBEM 2005. 18 th International Congress of Mechanical Engineering. November 6-11. Ouro Preto-MG.

Suzuki, H., Kasagi, N, and Suzuki, Y., 2000. "Active control of an axisymmetric jet with an intelligent nozzle", 1st Symposium on Turbulent Shear Flow Phenomena.
Townsend, A.A., 1976, "The Structure of Turbulent Shear Flow" Cambridge Univesity Press.
Urbin, G. and Metais, O., 1997. "Large-eddy simulations of three-dimensional spatially-developing round jes", in Direct and Large-Eddy Simulations 11, edited by Chollet, J.P.; Voke, P.R. and Kleiser, L. (Klumer Academic, New York).
Zaman, K.B.M.Q. and Hussain, A.K.M.F., 1980, "Vortex pairing in circular jet under controlled excitation. Part 1. General jet response", Journal of Fluid Mechanics 101, 449.
Zaman, K.B.M.Q., Reeder, M.F. and Samimy, M., 1994, "Control of an axisymmetric jet using vortex actuators", Physics Fluids 6, 778.

5. RESPONSIBILITY NOTICE

The authors are the only responsible for the printed material included in this paper.